Article

On the design of bubble columns equipped with a fine pore sparger: Effect of gas properties.

Athanasios G. Kanaris[1], Theodosios I. Pavlidis[2], Ariadni P. Chatzidafni[2] and Aikaterini A. Mouza*[2]

[1] Scientific Computing Department, STFC, Rutherford Appleton Laboratory, OX11 0QX, Didcot, UK.; agkanaris@gmail.com

[2] Department of Chemical Engineering, Aristotle University of Thessaloniki, Greece theodospi@auth.gr (T.I.P.); ariadni.chatzidafni@gmail.com (A.P.C.)

* Correspondence: mouza@auth.gr; Tel.: +30 2310 994161

Abstract: In our previous works we have proposed design equations that can predict with reasonable accuracy the transition point from homogeneous to heterogeneous regime as well as the gas holdup and the mean Sauter diameter at the homogeneous regime. The validity of the proposed correlations was checked with data obtained using different geometrical configurations and several Newtonian and non-Newtonian liquids as well as the addition of surfactants. However, in all the experiments the gas phase was atmospheric air. This work investigates the effect of gas phase properties by conducting experiments employing various gases (i.e., air, CO_2, He) that cover a wide range of physical property values. Experiments revealed that only the use of low-density gas (He) has a measurable effect on bubble column performance. More precisely, when the low-density gas (He) is employed, the transition point shifts to higher gas flow rates and the gas holdup decreases, a fact attributed to the lower momentum force exerted by the gas. In view of the new data, the proposed correlations have been slightly modified to include the effect of gas phase properties and it is found that they can predict the aforementioned quantities with an accuracy of ±15%. It has been also proved that CFD simulations are an accurate means for assessing the flow characteristics inside a bubble column.

Keywords: bubble column; porous sparger; holdup; bubble size; transition point; CFD

1. Introduction

Bubble columns are gas-liquid contactors that offer many advantages, due to their simple construction, low operating cost, high-energy efficiency and good mass transfer capabilities. Consequently, they are widely used in many industrial gas-liquid operations (e.g. gas/liquid reactions, agitation by gas injection, fermentations, waste water treatment, etc.) in chemical and biochemical industries. In all these processes, gas holdup and bubble size distribution are important design parameters, since they can be used to define the gas-liquid interfacial area available for mass transfer. In turn, these parameters depend strongly on the operating conditions, the physico-chemical properties of the two phases, the gas sparger type and the column geometry [1,2]. Depending on the gas flow rate, two main flow regimes can be readily observed in bubble columns, namely the ***homogeneous*** bubbly flow regime, which is encountered at relatively low gas velocities and the ***heterogeneous***

Peer-reviewed version available at ChemEngineering 2018, 2, 11; doi:10.3390/chemengineering2010011

(churn-turbulent flow) regime, which is observed for higher gas velocities. The *homogeneous* regime is characterized by discrete and uniformly dispersed bubbles. while in the *heterogeneous* regime the bubble interactions are more pronounced and lead to the formation of larger bubbles, which ascend with higher velocity. The homogeneous regime provides a larger interfacial contact area per unit mass of air and thus it is most desirable for practical applications [3], especially those involving sensitive materials (e.g. bioreactors, blood oxygenators) [4,5], since it also provides a low shear rate environment. The mechanism of bubble formation is of crucial importance to bubble column hydrodynamics. Figure 1 and Table 1 show the forces that act on an under-formation bubble (Eqs 1-6). A bubble is detached, when the sum of the upward forces (i.e. buoyancy, gas momentum, pressure) outweigh the sum of the downward ones (i.e. drag, inertial, surface tension).

In previous works conducted in this laboratory [2,6-8] we have experimentally studied the effect of the sparger characteristics (i.e. diameter, pore size), the liquid physical properties and the gas flow rate on the performance of a bubble column equipped with a fine pore sparger. We have employed both Newtonian and non-Newtonian liquids as well as liquids containing surfactants. Using the experimental data, we have formulated correlations that are based on dimensionless groups and can predict with reasonable uncertainty (better than ±15%) the transition point between the homogeneous and the heterogeneous regime as well as the gas hold-up and the bubble size distribution at the homogeneous regime. However, these correlations use data where the gas phase is air, although several bubble column applications use other gases (e.g. CO_2) and in this case the different gas density affects the amplitude of the forces that act on an under-formation bubble.

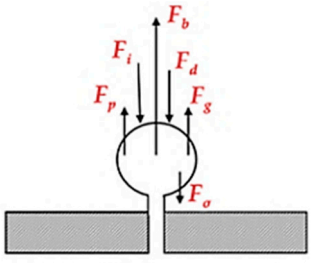

Figure 1. Forces acting on an under-formation bubble (Table 1).

Table 1. Forces acting during bubble formation.

Upward Forces	*Downward Forces*
Buoyancy	Drag
$F_b = (\rho_L - \rho_G) g V_b$ (1)	$F_d = \frac{1}{2}\rho_L W^2 \frac{\pi d_b^2}{4} C_D$ (4)
Gas momentum	Inertial
$F_G = \frac{\pi}{4} d_p^2 \rho_G W_G^2$ (2)	$F_i = \left(a_i + \frac{\rho_G}{\rho_L}\right) \rho_L V_b \gamma_b$ (5)
Pressure	Surface tension
$F_p = \frac{\pi}{4} d_p^2 (P_G - P_L)$ (3)	$F_\sigma = \pi d_p \sigma$ (6)

Thus, the purpose of this work is to check the validity of previously proposed correlations, by conducting experiments with several gases and, if necessary, to modify them to incorporate the effect

Peer-reviewed version available at ChemEngineering 2018, 2, 11; doi:10.3390/chemengineering2010011

of gas type. We will also use the experimental data to investigate the ability of a commercial CFD code to accurately simulate the performance of a bubble column and consequently to predict the flow characteristics (e.g. velocity profile, hold up distribution etc.) inside the column.

2. Experimental set-up and procedure

The experimental set-up (Figure 2) consists of a cylindrical bubble column, equipped with a fine pore sparger for the injection and the uniform distribution of the gas phase, an appropriate flowmeter for gas flow control, a high speed digital video camera (*Redlake MotioScope PCI® 1000S*) for bubble size and gas holdup measurements and a computer for acquiring and processing the data. A *Plexiglas®* rectangular box, filled with the same fluid as the one used at the corresponding experiment was placed around the bubble column to eliminate image distortion caused by light refraction.

The gas phase is introduced the column through a fine pore sparger, namely a 316 L SS porous disk (Mott Corp.®) with a nominal pore size of 40 μm or 100 μm, that covers the whole bottom plate. The effect of the sparger to column diameter ratio on the bubble column performance has been investigated and discussed in a previous paper [7]. To ensure that the gas phase is evenly distributed over the whole sparger area the gas phase was injected through a 1 cm nozzle to a vessel of 35 cm height placed beneath the bubble column, following the design proposed in a previous paper [7]. A recording rate of 125 frames per second (fps) was used for the measurement of gas holdup, while a speed of 500 fps was selected for measuring the bubble size.

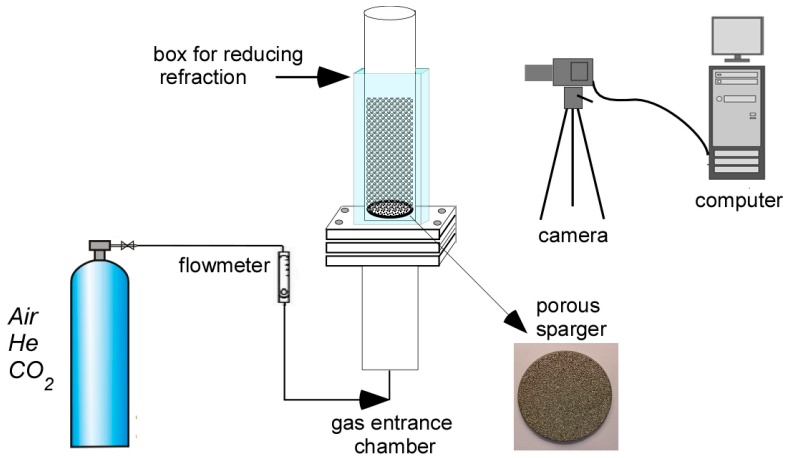

Figure 2. Experimental set-up.

The geometrical characteristics of the bubble columns studied are given in Table 2. The liquid phase was either de-ionized water or an aqueous glycerin solution (Table 3), while three gases, namely air, CO_2 and He, covering a sufficiently wide range of density values (Table 4) were individually employed. All the experiments were performed with no liquid throughput, at atmospheric pressure and ambient temperature conditions (i.e. around 20 C).

Preprints (www.preprints.org) | NOT PEER-REVIEWED | Posted: 5 February 2018 doi:10.20944/preprints201802.0027.v1

Peer-reviewed version available at ChemEngineering 2018, 2, 11; doi:10.3390/chemengineering2010011

Table 2. Bubble column characteristics.

d_C (cm)	d_S (cm)	d_P (μm)	d_P min (μm)	d_P max (μm)
5	5	100	5	500
9	9	40	3	70

Table 3. Liquid phase properties.

Liquid	ρ_L (Kg/m³)	μ_L (mPa·s)	σ_L (mN/m)
water	1000	1.0	72
aqueous glycerin 40 % v/v	1117	5.8	64

Table 4. Gas phase properties.

Gas	ρ_G (Kg/m³)	μ_G (10^{-5} Pa·s)
Air	1.39	1.8
CO_2	2.11	1.5
He	0.19	2.0

The average gas holdup (ε_G) is estimated by calculating the bed expansion as follows:

$$\varepsilon_G = \frac{\sum_{i=1}^{n} \varepsilon_{G,i}}{n} = \frac{\sum_{i=1}^{n} \frac{H_i - H_{o,i}}{H_i}}{n} = \frac{\sum_{i=1}^{n} \frac{\Delta H_i}{H_i}}{n} \quad (7)$$

where H_o and H is the liquid level before and after gas injection respectively, ΔH is the liquid level difference and n is the number of recurrent measurements for each gas flow rate (in this case n=5). The estimated maximum uncertainty of the measurements is less than 15%.From bubble images taken by the video camera the diameter of a sample of 100 bubbles was measured and the *Sauter* mean diameter (d_{32}), was calculated:

$$d_{32} = \frac{\sum_{i}^{N} n_i d_{bi}^3}{\sum_{i}^{N} n_i d_{bi}^2} \quad (8)$$

where d_{bi} and n_i are the diameter and the number of the bubbles of size class i respectively and N is the number of classes used for the distribution. The minimum number of classes required for the construction of the size distributions, k was estimated by the Sturges' rule:

$$k = 1 + log_2 S \quad (9)$$

where S is the sample size (~100 *bubbles*). The number of classes used for the construction of the distributions in the present work is 10 equal intervals.

Preprints (www.preprints.org) | NOT PEER-REVIEWED | Posted: 5 February 2018 doi:10.20944/preprints201802.0027.v1

Peer-reviewed version available at ChemEngineering 2018, 2, 11; doi:10.3390/chemengineering2010011

3. Results and discussion

3.1. Bubble size distribution

Figure 3 illustrates typical bubble size distributions with the 40 μm sparger (d_C=9 cm), for all gases studied and for a constant U_{GS} value. As expected [2], the distributions are log-normal while regardless of the liquid phase only the low density He gas exhibits an observable effect on the bubble distribution curve. This can be attributed to the considerably lower momentum force exerted by the low density He gas (Table 1). However, the value of mean Sauter diameter is not considerably affected by the type of gas but is mainly affected by the type of liquid phase employed (Table 5)

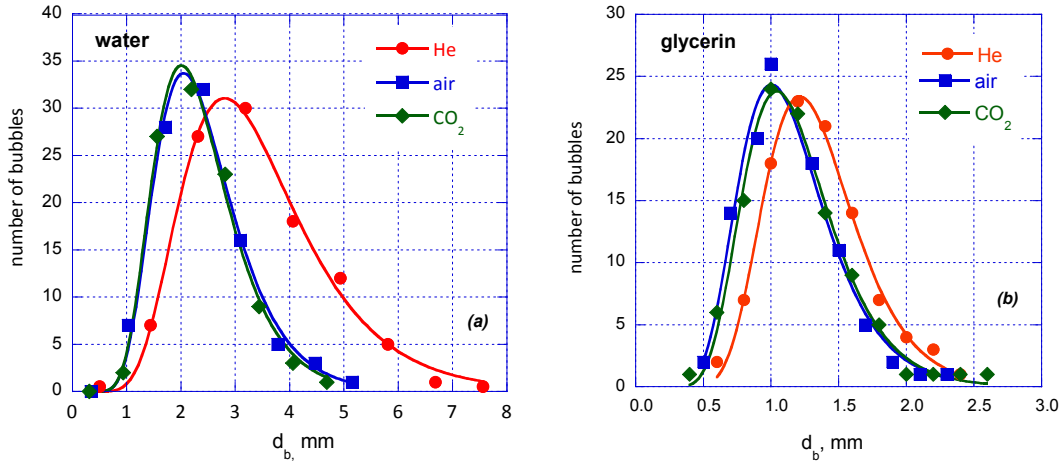

Figure 3. Effect of type of gas on bubble size distribution (U_{GS}=0.01 m/s.)

Table 5. Mean Sauter diameter (U_{GS}=0.01 m/s, d_P=40 μm).

liquid	*Gas*	*d_{32} (mm)*
water	Air	1.42
	He	1.50
	CO_2	1.40
aqueous glycerin solution 40%v/v	Air	1.16
	He	1.24
	CO_2	1.19

In previous works in our lab [2,7] a correlation for predicting the *Sauter* mean diameter (d_{32}) based on dimensionless numbers was proposed. The same correlation can be used for predicting the mean Sauter diameter when different gases are employed provided that the constants of the correlation are suitably adjusted (Eq. 10).

$$\frac{d_{32}}{d_s} = 0.9\left[We^{0.95}\, Re^{0.40}\, Fr^{0.47}\left(\frac{d_p}{d_s}\right)^{0.55}\right]^{0.51} \quad (10)$$

Preprints (www.preprints.org) | NOT PEER-REVIEWED | Posted: 5 February 2018 doi:10.20944/preprints201802.0027.v1

Peer-reviewed version available at ChemEngineering 2018, 2, 11; doi:10.3390/chemengineering2010011

where *We*, *Re* and *Fr* are the Weber, Reynolds and Froude number respectively, based on gas superficial velocity and liquid phase properties and defined as:

$$We = \frac{\rho_L U_{GS}^2 d_c}{\sigma_L} \tag{11}$$

$$Re = \frac{U_{GS} d_c \rho_L}{\mu_L} \tag{12}$$

$$Fr = \frac{U_{GS}^2}{d_c g} \tag{13}$$

In Figure 4 it is shown that the proposed correlation (Eq. 10) can be used for predicting d_{32} values with reasonable accuracy (i.e. ±15%) for all the gases employed.

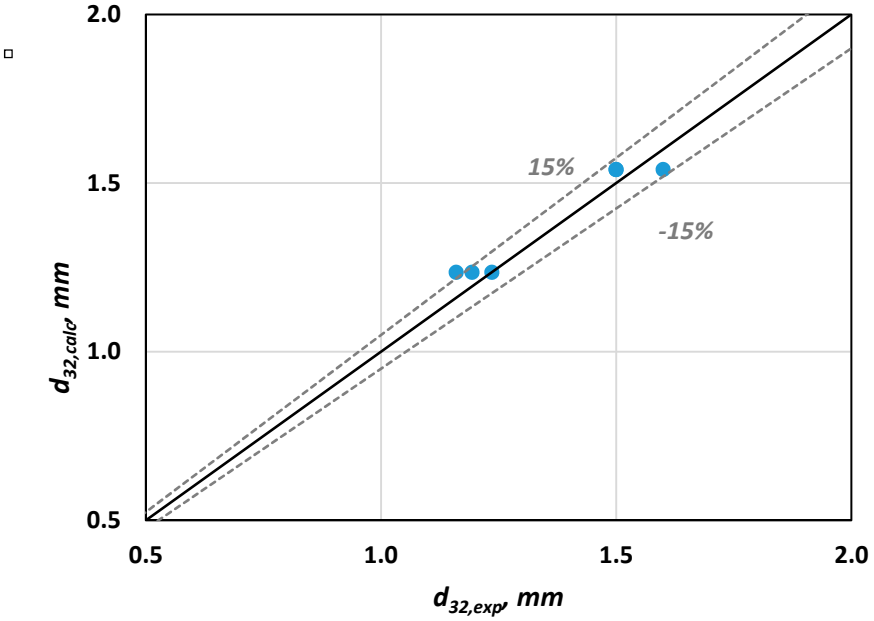

Figure 4. Comparison of the *Sauter* mean diameter prediction with experimental data (Table 5) (U_{GS}=0.01 m/s, d_p=40 μm, d_c=9 cm).

3.2. *Regime transition*

The transition point from homogeneous to heterogeneous regime is estimated by applying the *drift flux analysis*, which considers the relative motion of the two phases [9]. The basic quantity is the drift flux, *j*, is given by:

$$j = U_{GS}(1-\varepsilon_G) \tag{14}$$

where ε_G is the gas holdup *and* U_{GS} is the superficial gas velocity defined as:

$$U_{GS} = \frac{Q_G}{A} \tag{15}$$

where Q_G is the gas flow rate and *A* the column cross section. When the drift flux is plotted versus the gas holdup, the change in the slope of the curve indicates the transition from homogeneous to heterogeneous regime [10].

Preprints (www.preprints.org) | NOT PEER-REVIEWED | Posted: 5 February 2018 doi:10.20944/preprints201802.0027.v1

Peer-reviewed version available at ChemEngineering 2018, 2, 11; doi:10.3390/chemengineering2010011

The effect of the type of gas on regime transition is illustrated in Figure 5. It is obvious that, only when the lower density gas, He, is employed, the homogeneous regime is extended to higher j or equally U_{GS} values.

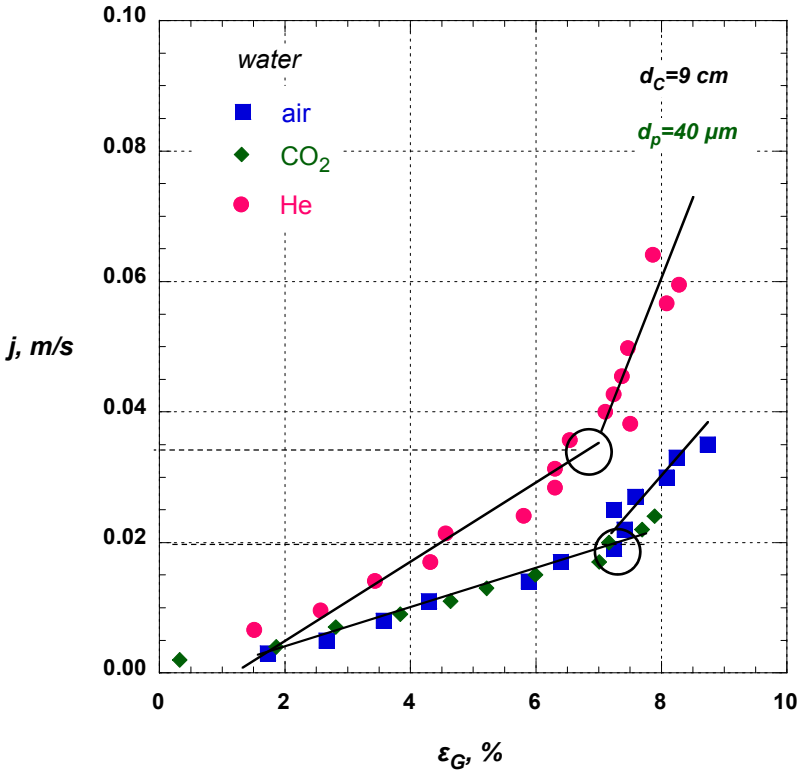

Figure 5. Effect of type of gas on regime transition for water (d_p=40 μm, d_c=9 cm).

In previous papers [7,11] we have proposed a correlation (Eq. 12) for predicting the transition point that is based on dimensionless numbers and incorporates the physical properties of the liquid phase as well as the geometrical characteristics of the column and the porous sparger. This correlation has the general form:

$$Fr_{trans} = a_1 \left[Eo^{a_2} \left(\frac{d_s}{d_c} \right)^{a_3} \right]^{a_4} \tag{16}$$

where Fr_{trans} is the Froude number at the transition point and Eo the Eotvos number based on d_{32}:

$$Fr_{trans} = \frac{U_{GS,trans}^2}{d_p g} \tag{17}$$

$$Eo = \frac{d_{32}^2 \rho_L g}{\sigma_L} \tag{18}$$

In view of the new results to incorporate the effect of type of gas, the ratio of gas density to that of air density is added. The new correlation is as follows:

Preprints (www.preprints.org) | NOT PEER-REVIEWED | Posted: 5 February 2018 doi:10.20944/preprints201802.0027.v1

Peer-reviewed version available at ChemEngineering 2018, 2, 11; doi:10.3390/chemengineering2010011

$$Fr_{trans} = 1.2\left[Eo^{0.001}\left(\frac{d_S}{d_C}\right)^{0.02}\left(\frac{\rho_G}{\rho_{air}}\right)^{0.5}\right]^{0.005} \quad (19)$$

The predicted $U_{GS,\,trans}$ values are in very good agreement, i.e. better than 15%, with the corresponding experimental data. The proposed correlation is suitable for predicting the transition point from homogeneous to heterogeneous regime.

3.3. *Gas holdup*

In this section the effect of the various parameter on the gas hold-up values is investigated. As it is expected, gas holdup increases with the gas velocity. The first part of the curve corresponds to the homogeneous regime. A transition regime follows where a slight decrease in gas holdup is observed. Finally, at the heterogeneous regime the gas holdup continues to increase, but with a lower slope than the homogeneous regime [6].

Figure 6 shows the dependence of gas holdup on corresponding gas superficial velocity for the two bubble columns used. It is obvious from that by increasing the column diameter the gas holdup increases, especially for higher gas flow rates. However, the literature results concerning the effect of column diameter on gas holdup are contradictory. Some researchers report that the column diameter has no effect on gas holdup [12-15]. The above works concern bubble columns with diameter larger than 10 cm, where the gas distributor is a perforated plate.

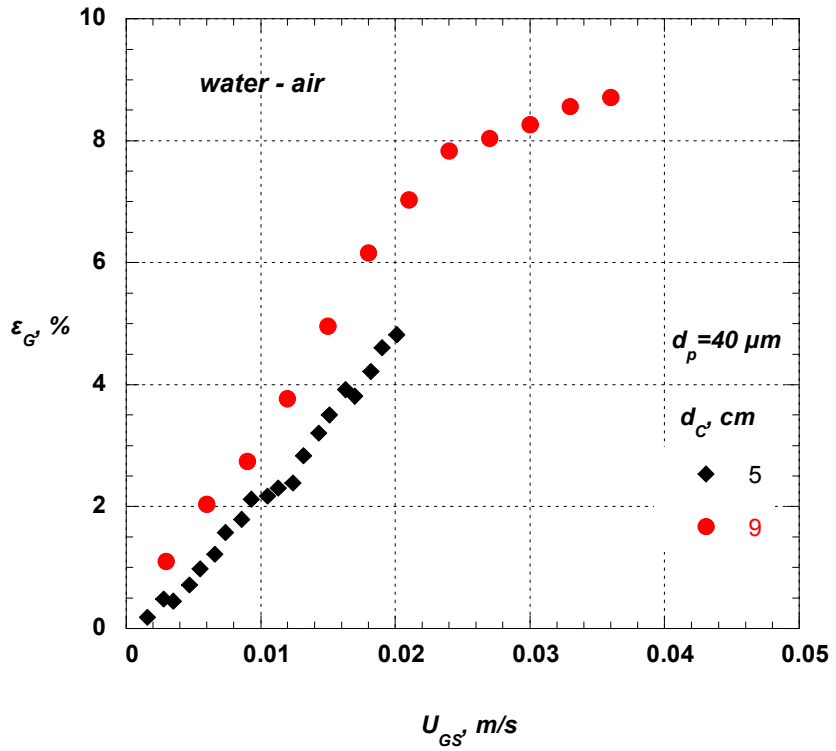

Figure 6. Effect of column diameter on gas holdup for the water-air system (d_p=40 μm).

Ruzicka et al. [16] also state that the gas holdup is independent of column dimensions provided that the column diameter is larger than 10 cm, the column height is larger than 15 cm and the column height to diameter ratio is more than 5. On the other hand, some works report that the column diam-

Peer-reviewed version available at ChemEngineering 2018, 2, 11; doi:10.3390/chemengineering2010011

eter affects the gas holdup. Botton et al. [17] report that gas holdup increases when the column diameter decreases, whereas Kumar et al. [18] who conducted experiments in bubble columns with diameters larger than 10 cm, state that there is a continuous increase in the gas holdup with increasing column diameter. To the best of our knowledge, there are no experimental results concerning bubble columns with diameter less than 10 cm, equipped with fine porous sparger. Dhotre et al. [19], who have numerically studied the effect of sparger type and height to diameter ratio on radial gas holdup profiles, report that for multipoint spargers, an increase of the column height to column diameter ratio results into marginal decrease of gas holdup. Obviously, when the column diameter decreases the wall effects become more intense.

Figure 7 presents typical effect of the type of gas on gas holdup. With increasing gas density gas holdup increases, e.g. helium that has a lower density exhibits lower values of gas holdup than air and CO_2. This behavior is attributed to the fact that, the lower density gas exerts a lower momentum force to an under-formation bubble (Eq. 2). This observation agrees with other researchers [20,21] who also reported that gases of higher density produce higher gas holdup values, attributing this behavior on phenomena occurring during bubbles formation on the sparger. However, it is worth noticing that, even though the density of CO_2 is 50% higher than that of atmospheric air, for the lower gas superficial velocities both air and CO_2 exhibit almost the same behavior and only when the density decreases by more than 80% (i.e. for He)) a noticeable change is observed (Figure 7)

In previous studies conducted in our lab [6,7,11] a correlation for predicting the average gas holdup, ε_G, was proposed based on dimensionless numbers. The equation has the general form:

$$\varepsilon_G = c_1 \left[Fr^{c_2} Ar^{c_3} Eo^{c_4} \left(\frac{d_s}{d_c} \right)^{c_5} \left(\frac{d_p}{d_s} \right)^{c_6} \right]^{c_7} \tag{20}$$

where Fr, Ar and Eo are the dimensionless Froude, Archimedes and Eotvos number respectively defined by:

$$Fr = \frac{U_{GS}^2}{d_c g} \tag{21}$$

$$Ar = \frac{d_C^3 \rho_L^2 g}{\mu_L^2} \tag{22}$$

$$Eo = \frac{d_c^2 \rho_L g}{\sigma_L} \tag{23}$$

the quantities d_c, d_s, are the column and the sparger diameter, while d_p is the mean pore size of the sparger material. The values of constants c_1 to c_7 depend on the of liquid phase. It was also proved [6-8,11] that the proposed correlations can predict hold up with reasonable accuracy, i.e. better than 15%.

However, in the ε_G prediction the type of gas is not taken into account although the gas momentum affects bubble evolution (Table 1). From Figure 7, where the effect of gas type is presented, it is apparent that only the very low density gas He has has a measurable effect on gas

Preprints (www.preprints.org) | NOT PEER-REVIEWED | Posted: 5 February 2018 doi:10.20944/preprints201802.0027.v1

Peer-reviewed version available at ChemEngineering 2018, 2, 11; doi:10.3390/chemengineering2010011

hold-up value. In case that the gas phase is other than air, it is necessary to introduce a term that incorporates the properties of the gas phase.

Based on the above, we have modified Eq. 16 by introducing in the gas Reynolds number Re_G defined as:

$$Re = \frac{U_{GS} d_C \rho_G}{\mu_G} \tag{24}$$

The modified form of the proposed correlation is as follows:

$$\varepsilon_G = c_1 \left[Fr^{c_2} Ar^{c_3} Eo^{c_4} Re_G^{c_5} \left(\frac{d_s}{d_C} \right)^{c_6} \left(\frac{d_p}{d_s} \right)^{c_7} \right]^{c_8} \tag{25}$$

Where the constants of the correlation are given in Table 6.

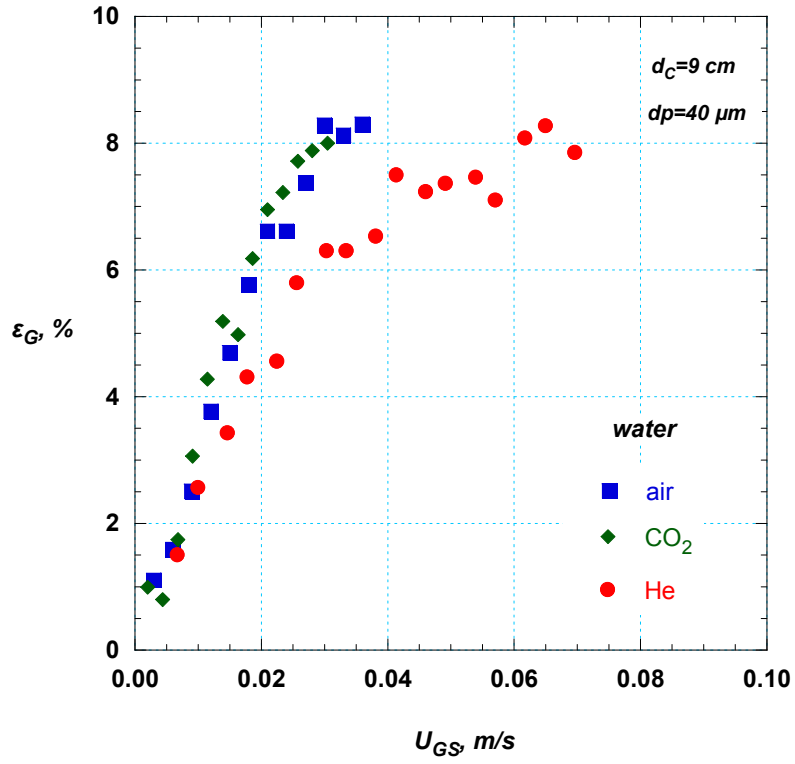

Figure 7. Effect of type of gas on gas holdup (d_p=40 μm, d_c=9 cm).

Table 6: Constants value for ε_G prediction equation (Eq. 25).

C_1	C_2	C_3	C_4	C_5	C_6	C_7	C_8
0.020	0.300	0.015	3.50	0.043	1.10	2.62	1.18

Figure 8 shows that the ε_G values predicted by Eq. 25 are in very good agreement (±15%) with the corresponding experimental data.

Preprints (www.preprints.org) | NOT PEER-REVIEWED | Posted: 5 February 2018 doi:10.20944/preprints201802.0027.v1

Peer-reviewed version available at ChemEngineering 2018, 2, 11; doi:10.3390/chemengineering2010011

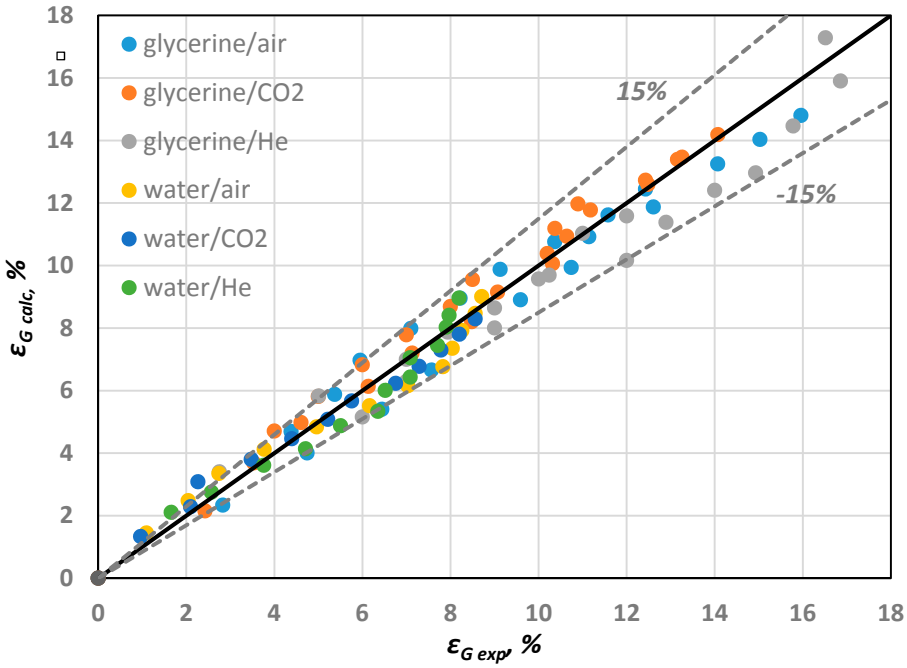

Figure 8. Comparison of the proposed correlation with the experimental data.

4. Numerical Simulations

A method to gain more knowledge and detailed physical understanding of the hydrodynamics in bubble columns is the use of Computational Fluid Dynamics (CFD). CFD can be regarded as an effective tool to clarify the importance of physical effects (e.g. gravity, surface tension) on flow by adding or removing them at will. An increasing number of papers deal with CFD application to bubble columns [1,7]. Vial et al. [22] cite the most important reasons for this increasing interest. In this paper our intension is to validate the CFD code by comparing the numerical results with relevant experimental data. Then using the validate code we will be able to visualize the flow field inside the column.

The commercial CFD code ANSYS CFX 18.1, which was employed for the simulations, incorporates the MUSIG (Multiple Size Group) model to handle polydisperse multiphase flows, i.e., flows where the dispersed phase has wide size variation. In this case, the different sizes of the bubbles interact with each other through mechanisms of breakup and coalescence [23]. MUSIG starts by using the population balance equation to estimate the birth and death rates of bubbles due to breakup and coalescence. It requires the equation to use discretised size groups, whose initial conditions are provided by the user. In those size groups, the equal diameter discretisation assumption is considered: the diameter represented by the group boundary is assumed to be midway between the diameters represented by the adjacent groups. The mass represented by the upper limit of the largest-size group is based on the diameter represented by that limit, and the mass represented by the lower limit of the smallest-size group is assumed to be zero. MUSIG combines the population balance method with the break-up [24] and coalescence [25] models, to predict the bubble size distribution of the dispersed phase. It also uses the Eulerian-Eulerian two-phase model, and for the type of flow encountered in a bubble column, it is recommended to use the k-ε turbulent model for the continuous phase, while the dispersed phase is simulated with the zero-equation model. More details on the computational methods used are given in previous work by the authors [26].

Preprints (www.preprints.org) | NOT PEER-REVIEWED | Posted: 5 February 2018 doi:10.20944/preprints201802.0027.v1

Peer-reviewed version available at ChemEngineering 2018, 2, 11; doi:10.3390/chemengineering2010011

All simulations were performed in time-dependent, transient mode, for the same total time length, i.e., 20 s. Due to the high computational demand, a parallel computing system was used, utilizing 24 AMD Opteron cores with 64 GB RAM. To ensure the accuracy of the results, a grid-dependence and a timestep-dependence study were performed for the higher air velocity tested. Gas holdup values were calculated for different grid size meshes up to 800,000 nodes, and for timesteps as small as 800 ms. It was found that the results are not significantly influenced by the timestep variation, while for grid densities more than 700,000 nodes gas holdup value is practically the same, thus this grid density was used for the remaining simulations, and a timestep of 800 ms was also used.

The simulations were validated by comparing the calculated hold-up values with the relevant experimental ones. From Table 7, where representative CFD results are presented, it is clear that the numerical simulation can quite accurately predict the hold up, i.e. achieving a deviation of less than 5%.

Table 7. Comparison of typical simulation results with the experimental data.

Liquid phase	*Gas phase*	U_{GS}, *m/s*	$\varepsilon_{G\ exp}$, *%*	$\varepsilon_{G\ calc}$, *%*	*deviation %*
water	He	0.02	5.9	5.6	5.0
		0.03	6.6	6.4	2.6
water	air	0.02	6.5	6.2	4.5
		0.03	7.9	8.0	0.7
aqueous glycerin 40% v/v	He	0.02	8.4	8.0	5.0

In Figure 9 typical CFD results concerning the evolution of gas volume fraction inside the bubble column (i.e. the bed expansion) is presented. The calculated gas hold-up values given in Table 6 were predicted by calculating the liquid bed expansion.

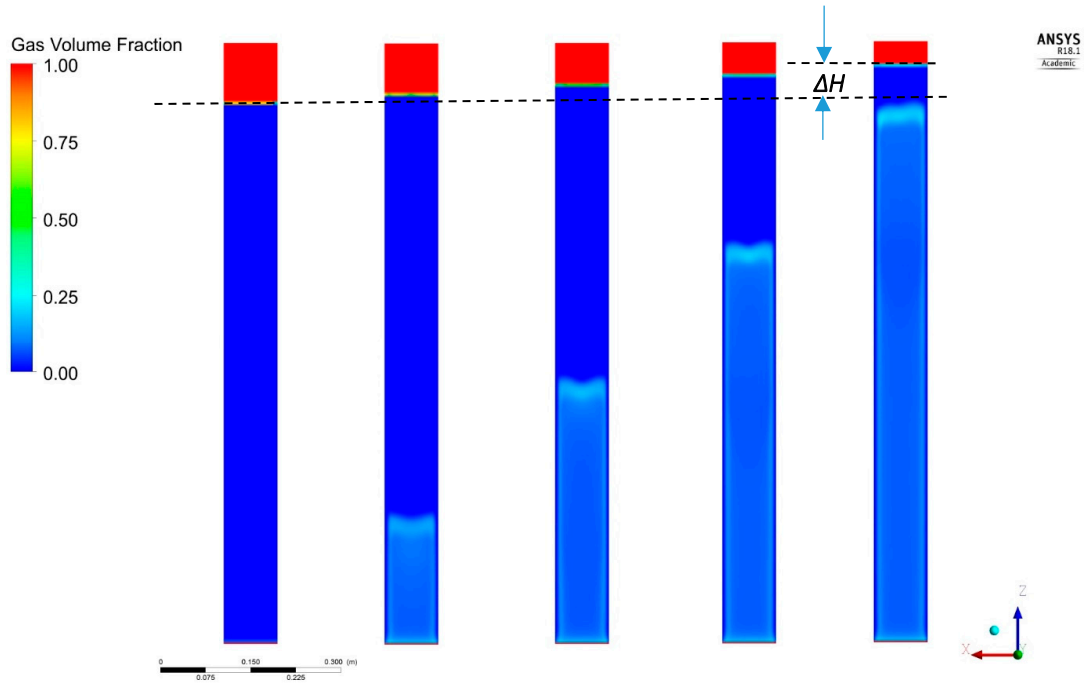

Figure 9. Bed expansion *(ΔH)* for different time snapshots: *t*=0, 0.8, 1.6, 2.4 and 3.2 s (air-water, U_{GS}=0.2 m/s d_p=40 μm, d_c=9 cm).

Preprints (www.preprints.org) | NOT PEER-REVIEWED | Posted: 5 February 2018 doi:10.20944/preprints201802.0027.v1

Peer-reviewed version available at ChemEngineering 2018, 2, 11; doi:10.3390/chemengineering2010011

Figure 10 also presents typical contour plots at a randomly selected time snapshot, offering an insight on the expected distribution of shear stress of the liquid phase and streamlines formation.

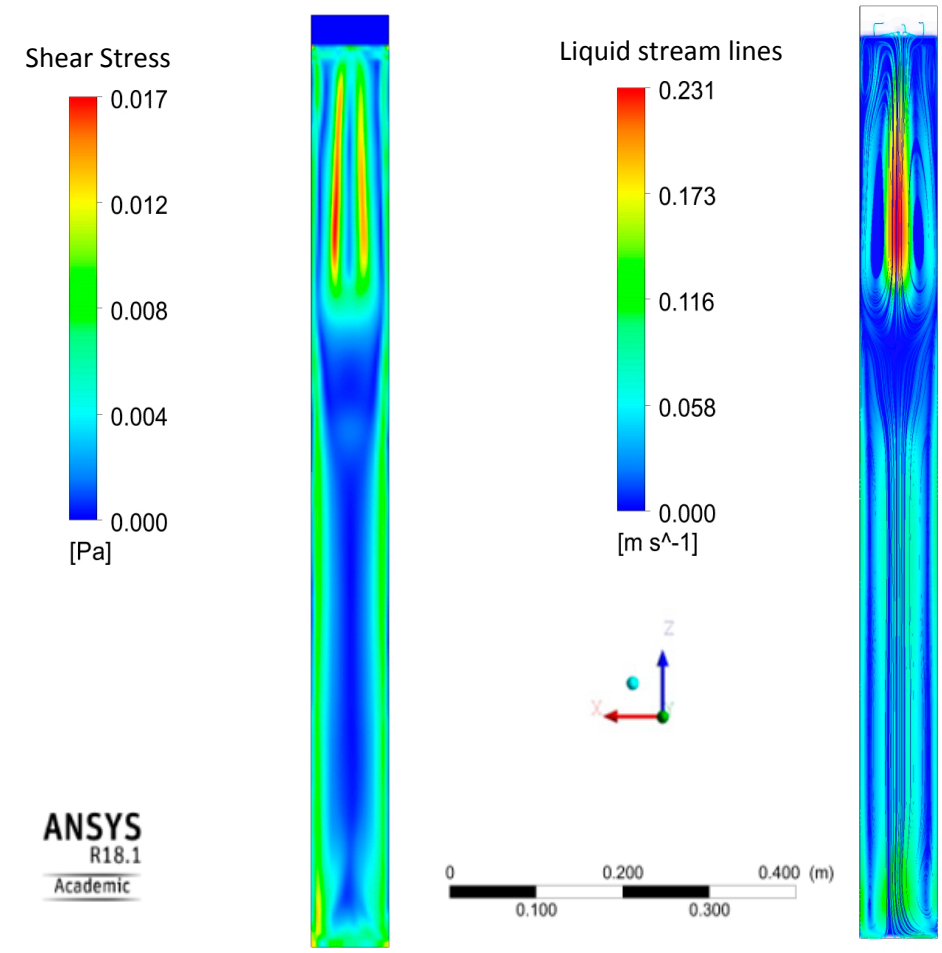

Figure 10. Typical CFD results at the middle plane of the bubble column: a) Shear stress distribution; b) Streamlines colored with the liquid phase velocity (t=5.8 s, U_{GS}=0.2 m/s, air-water, d_p=40 μm, d_c=9 cm).

5. Concluding remarks

In this work, we have experimentally investigated in what extent the type of gas phase influences the performance of a bubble column reactor by employing gases that cover a fairly wide range of physical properties; namely atmospheric air, CO_2 exhibit almost the same behavior, while the low density He shows a measurable effect on bubble column design quantities. This can be attributed to the fact that the low density He gas exhibits a lower momentum force. Thus, the previously proposed correlations for predicting the transition point from the homogeneous to the heterogeneous regime, the gas holdup and the *Sauter* mean diameter are slightly modified to include the effect of the type of gas employed. The new correlations can predict the aforementioned quantities with reasonable accuracy (better than 15%). Relevant CFD simulations were also performed and validated with the available experiments results in terms of gas hold-up. Thus, it has been demonstrated that CFD can be used for predicting the flow characteristics that are generally difficult to be experimentally measured but are essential during bubble column design, as for example the shear stress or the velocity distribution.

Nomenclature

A	column cross section, m^2
d_b	bubble diameter, m
d_{32}	*Sauter* mean diameter, m
d_C	column diameter, m
d_p	pore diameter, m
d_S	sparger diameter, m
F_b	buoyancy force, N
F_d	drag force, N
F_g	gas momentum force, N
F_i	inertial force, N
F_p	pressure force, N
F_σ	surface tension force, N
g	acceleration of gravity, m/s^2
H_C	column height, m
j	drift flux, m/s
Q_G	gas flow rate, m^3/s
U_{GS}	superficial gas velocity, m/s
W_g	bubble formation velocity, m/s

Greek letters

ε_G	average gas holdup, dimensionless
μ_G	gas phase viscosity Pa s
μ_L	liquid phase viscosity, Pa s
ρ_G	gas density, Kg/m^3
ρ_L	liquid density, Kg/m^3
σ_L	surface tension, mN/m

Dimensionless quantities

Ar	Archimedes number
Eo	Eotvos number
Fr	Froude number
Fr_{tans}	Froude number at transition point
k	minimum number of classes
N	number of classes used for the distributions
n_i	number of bubbles of size class i
Re	Reynolds number based on liquid properties
Re_G	Reynolds number based on gas properties
S	sample size
We	Weber number

Acknowledgments: The authors would like to thank Asterios Lekkas for the construction and installation of the experimental setup and Spiros V. Paras for his constructive comments.

Author Contributions: A.A. Mouza had the initial conception of this work and designed the experiments; T.I. Pavlidis and A.P. Chatzidafni conducted the experiments, acquired and analyzed the data; A.G. Kanaris and A.A. Mouza performed the simulations; A.A. Mouza interpreted the results and wrote the manuscript. This work is not affiliated with the Science and Technology Facilities Council (STFC).

Conflicts of Interest: The authors declare no conflict of interest.

References

1. Camarasa, E.; Vial, C. Influence of coalescence behaviour of the liquid and of gas sparging on hydrodynamics and bubble characteristics in a bubble column. Chemical Engineering and Processing: Process Intensification 1999, 38, 329-344, https://doi.org/10.1016/S0255-2701(99)00024-0.
2. Kazakis, N.A.; Mouza, A.A.; Paras, S.V. Experimental study of bubble formation at metal porous spargers: Effect of liquid properties and sparger characteristics on the initial bubble size distribution. Chemical Engineering Journal 2008, 137, 265-281, DOI 10.1016/j.cej.2007.04.040.
3. Joshi, J.B.; Vitankar, V.S. Coherent flow structures in bubble column reactors. Chemical Engineering Science 2002, 57, 3157-3183, https://doi.org/10.1016/S0009-2509(02)00192-6.
4. Dhanasekharan, K.M.; Sanyal, J. A generalized approach to model oxygen transfer in bioreactors using population balances and computational fluid dynamics. Chemical Engineering Science 2005, 60, 213-218, https://doi.org/10.1016/j.ces.2004.07.118.
5. Jones, T.J.; Deal, D.D. How effective are cardiopulmonary bypass circuits at removing gaseous microemboli? J Extra Corpor Technol 2002, 34, 34-9
6. Mouza, A.A.; Dalakoglou, G.K.; Paras, S.V. Effect of liquid properties on the performance of bubble column reactors with fine pore spargers. Chemical Engineering Science 2005, 60, 1465-1475, DOI 10.1016/j.ces.2004.10.013.
7. Passos, A.D.; Voulgaropoulos, V.P.; Paras, S.V.; Mouza, A.A. The effect of surfactant addition on the performance of a bubble column containing a non-Newtonian liquid. Chemical Engineering Research and Design 2015, 95, 93-104, https://doi.org/10.1016/j.cherd.2015.01.008.
8. Anastasiou, A.D.; Kazakis, N.A.; Mouza, A.A.; Paras, S.V. Effect of organic surfactant additives on gas holdup in the pseudo-homogeneous regime in bubble columns equipped with fine pore sparger. Chemical Engineering Science 2010, 65, 5872-5880, DOI 10.1016/j.ces.2010.08.011.
9. Isbin, H.S. One-dimensional two-phase flow, Graham B. Wallis, McGraw-Huill, New York (1969). AIChE Journal 1970, 16, 896-1105, 10.1002/aic.690160603.
10. Shah, Y.T.; Kelkar, B.G. Design parameters estimations for bubble column reactors. AIChE Journal 1982, 28, 353-379, 10.1002/aic.690280302.
11. Kazakis, N.A.; Papadopoulos, I.D.; Mouza, A.A. Bubble columns with fine pore sparger operating in the pseudo-homogeneous regime: Gas hold up prediction and a criterion for the transition to the heterogeneous regime. Chemical Engineering Science 2007, 62, 3092-3103, DOI 10.1016/j.ces.2007.03.004.
12. Yovel, Y.; Franz, M.O. Plant classification from bat-like echolocation signals. PLoS Computational Biology 2008, 4, e1000032, DOI 10.1371/journal.pcbi.1000032.
13. Forret, A.; Schweitzer, J.M. Influence of scale on the hydrodynamics of bubble column reactors: an experimental study in columns of 0.1, 0.4 and 1m diameters. Chemical Engineering Science 2003, 58, 719-724, https://doi.org/10.1016/S0009-2509(02)00600-0.

14. Wilkinson, P.M.; Spek, A.P.; van Dierendonck, L.L. Design parameters estimation for scale-up of high-pressure bubble columns. AIChE Journal 1992, 38, 544-554, 10.1002/aic.690380408.
15. Vatai, G.Y..Tekić, M.N. Gas hold-up and mass transfer in bubble columns with pseudoplastic liquids. Chemical Engineering Science 1989, 44, 2402-2407, https://doi.org/10.1016/0009-2509(89)85178-4.
16. Ruzicka, M.C.; Drahoš, J. Effect of bubble column dimensions on flow regime transition. Chemical Engineering Science 2001, 56, 6117-6124, https://doi.org/10.1016/S0009-2509(01)00215-9.
17. Botton, R.; Cosserat, D.; Charpentier, J.C. Influence of column diameter and high gas throughputs on the operation of a bubble column. The Chemical Engineering Journal 1978, 16, 107-115, https://doi.org/10.1016/0300-9467(78)80051-3.
18. Kumar, S.B.; Moslemian, D.; Duduković, M.P. Gas-holdup measurements in bubble columns using computed tomography. AIChE Journal 1997, 43, 1414-1425, 10.1002/aic.690430605.
19. Dhotre, M.T.; Ekambara, K.; Joshi, J.B. CFD simulation of sparger design and height to diameter ratio on gas hold-up profiles in bubble column reactors. Experimental Thermal and Fluid Science 2004, 28, 407-421, https://doi.org/10.1016/j.expthermflusci.2003.06.001.
20. Hecht, K.; Bey, O. Effect of Gas Density on Gas Holdup in Bubble Columns. Chemie Ingenieur Technik 2015, 87, 762-772, 10.1002/cite.201500010.
21. Krishna, R.; Wilkinson, P.M.; Van Dierendonck, L.L. A model for gas holdup in bubble columns incorporating the influence of gas density on flow regime transitions. Chemical Engineering Science 1991, 46, 2491-2496, https://doi.org/10.1016/0009-2509(91)80042-W.
22. Vial, C.; Lainé, R. Influence of gas distribution and regime transitions on liquid velocity and turbulence in a 3-D bubble column. Chemical Engineering Science 2001, 56, 1085-1093, https://doi.org/10.1016/S0009-2509(00)00325-0.
23. ANSYS. CFX-Solver Theory Guide, 2017.
24. Luo, H..Svendsen, H.F. Theoretical model for drop and bubble breakup in turbulent dispersions. AIChE Journal 1996, 42, 1225-1233, 10.1002/aic.690420505.
25. Prince, M.J..Blanch, H.W. Bubble coalescence and break-up in air-sparged bubble columns. AIChE Journal 1990, 36, 1485-1499, 10.1002/aic.690361004.
26. Mouza, A.A.; Kazakis, N.A.; Paras, S.V. Bubble column reactor design using a CFD code, in 1st Intern. Conference "From scientific computing to computational engineering" 2004: Athens, Greece.